THE JOURNAL OF BIOLOGICAL CHEMISTRY VOL. 286, NO. 17, pp. 15317–15331, April 29, 2011

Seeding of Normal Tau by Pathological Tau Conformers Drives Pathogenesis of Alzheimer-like Tangles*[S]

Received for publication, December 4, 2010, and in revised form, March 3, 2011 Published, JBC Papers in Press, March 3, 2011, DOI 10.1074/jbc.M110.209296

Jing L. Guo and Virginia M.-Y. Lee[1]

From the Department of Pathology and Laboratory Medicine, Institute on Aging and Center for Neurodegenerative Disease Research, University of Pennsylvania School of Medicine, Philadelphia, Pennsylvania 19104

Neurofibrillary tangles (NFTs) in Alzheimer disease and related tauopathies are composed of insoluble hyperphosphorylated Tau protein, but the mechanisms underlying the conversion of highly soluble Tau into insoluble NFTs remain elusive. Here, we demonstrate that introduction of minute quantities of misfolded preformed Tau fibrils (Tau pffs) into Tau-expressing cells rapidly recruit large amounts of soluble Tau into filamentous inclusions resembling NFTs with unprecedented efficiency, suggesting a "seeding"-recruitment process as a highly plausible mechanism underlying NFT formation *in vivo*. Consistent with the emerging concept of prion-like transmissibility of disease-causing amyloidogenic proteins, we found that spontaneous uptake of Tau pffs into cells is likely mediated by endocytosis, suggesting a potential mechanism for the propagation of Tau lesions in tauopathy brains. Furthermore, sequestration of soluble Tau by pff-induced Tau aggregates attenuates microtubule overstabilization in Tau-expressing cells, supporting the hypothesis of a Tau loss-of-function toxicity in cells harboring NFTs. In summary, our study establishes a cellular system that robustly develops authentic NFT-like Tau aggregates, which provides mechanistic insights into NFT pathogenesis and a potential tool for identifying Tau-based therapeutics.

Neurodegenerative tauopathies, including Alzheimer disease (AD)[2] and frontotemporal dementias, are characterized by neurofibrillary tangles (NFTs) composed of intracellular hyperphosphorylated Tau aggregates (1–4). Predominantly expressed in neurons, Tau is a microtubule (MT)-binding protein that stabilizes and promotes the assembly of MTs (5, 6), and the Tau-MT interactions are negatively regulated by phosphorylation of Tau (7, 8). In adult brains, alternative splicing of the *MAPT* gene (9, 10) generates six Tau isoforms containing either three or four MT-binding repeats (3R or 4R Tau) and 0–2 N-terminal inserts (0N, 1N, or 2N Tau).

A naturally unfolded soluble protein under normal conditions, Tau acquires highly ordered β-pleated sheet structures as it assembles into insoluble, hyperphosphorylated 15–20 nm in diameter paired helical filaments as well as less frequent straight filaments that constitute NFTs in AD and related tauopathies (11, 12). Mechanisms underlying such dramatic conversions remain a conundrum. Significant correlations of total NFT burden with cognitive decline are observed in AD patients (13, 14), and importantly, discoveries of over 30 dominantly inherited mutations in the *MAPT* gene in frontotemporal dementia with parkinsonism linked to chromosome 17 (FTDP-17) (15–18) strongly suggest a causal link between Tau abnormality and neuronal dysfunction. Although the exact mechanisms of Tau-mediated neurodegeneration are not well understood, both the loss of the MT-binding function of Tau due to sequestration of soluble Tau into tangles and the toxic gains of function because of the sheer physical occupancy of large intracellular aggregates have been proposed to explain the dire consequences of Tau aggregation (19, 20).

A cellular system recapitulating features of tauopathies would provide a useful tool to study the cause and consequences of Tau aggregation. However, because Tau is a highly soluble protein, overexpressed Tau resists aggregation despite spontaneous hyperphosphorylation in most cell lines. Moreover, high expression of Tau overstabilizes MTs and inhibits cell division, and it is therefore not well tolerated by dividing cultured cells (21, 22). Thus, our current understanding of Tau fibrillization has relied on studies using cell-free systems in which the formation of Tau amyloid fibrils is greatly enhanced by polyanionic factors (23–25). It has been shown that the MT-binding repeats of Tau are both necessary and sufficient for *in vitro* fibrillization, and the repeat domain alone assembles into fibrils more readily than full-length Tau (26). Importantly, Tau fibril assembly occurs by a nucleation-dependent mechanism, whereby the formation of oligomeric intermediates constitutes an initial lag phase followed by a relatively rapid elongation phase (27). Therefore, "seeding" Tau fibrillization reactions with preformed Tau fibrils (Tau pffs) can bypass the rate-limiting nucleation step and accelerate fibrillization of monomeric Tau. We hypothesized that similar seeding strategies could be employed to promote Tau aggregation in cultured cells, and in fact, several recent cell culture studies have demonstrated induction of intracellular aggregates by exogenously derived amyloid fibrils from several disease proteins involved in neurodegenerative disorders, including Tau (28–31). Moreover, two recent studies on transgenic mice demonstrated the induction of WT Tau pathology by injection of brain extracts containing mutant Tau aggregates (32) or by expression of truncated Tau that is aggregation-prone (33), exemplifying the *in vivo* rele-

* This work was supported, in whole or in part, by National Institutes of Health Grant AG17586. This work was also supported by Cure Alzheimer Fund.

[S] The on-line version of this article (available at http://www.jbc.org) contains supplemental Figs. 1–5, Table 1, and additional references.

[1] To whom correspondence should be addressed: 3rd Floor, Maloney Bldg., 3600 Spruce St., Philadelphia, PA 19104-4283. Tel.: 215-662-6427; Fax: 215-349-5909; E-mail: vmylee@upenn.edu.

[2] The abbreviations used are: AD, Alzheimer disease; Ac-tub, acetylated tubulin; FTDP-17, frontotemporal dementias with Parkinsonism linked to chromosome 17; mAb, monoclonal antibody; MT, microtubule; NFT, neurofibrillary tangle; pff, preformed fibril; ThS, thioflavin S; WGA, wheat germ agglutinin; Ab, antibody.

vance of seeded aggregation of Tau. However, although two previous studies claimed to have demonstrated the recruitment of soluble Tau into insoluble aggregates in cultured cells (29, 31), it is unclear if these Tau aggregates resemble NFTs. Here, we provide unequivocal evidence for the seeding phenomenon in cultured cells by demonstrating high efficiency recruitment of soluble Tau into authentic NFT-like aggregates. Furthermore, the establishment of a cellular system with a significant number of NFT-like aggregates enables investigation on the pathological mechanisms of Tau tangle formation as well as cellular transmission of pathological Tau, which are more difficult to study in animal models.

EXPERIMENTAL PROCEDURES

Reagents and Antibodies—BioPORTER® Quikease™ protein delivery kit for fibril transduction, wheat germ agglutinin (WGA), and *N*-acetylglucosamine (GlcNAc) were purchased from Sigma. Antibodies used in this study are listed and described in supplemental Table 1.

Recombinant Tau Purification and in Vitro Fibrillization—The cDNAs coding for 1) the longest isoform of Tau (2N4R) with a Myc tag at the 3′ end (3′Myc-T40), 2) truncated Tau containing only four MT-binding repeats with a Myc tag at the 5′ end (5′Myc-K18), and 3) 5′Myc-K18 containing P301L mutation (5′Myc-K18/P301L) were cloned into NdeI/EcoRI sites in pRK172 bacterial expression vector. Each protein was expressed in BL21 (DE3) RIL cells and purified by cationic exchange using a fast protein liquid chromatography (FPLC) column as described previously (34). *In vitro* fibrillization was conducted by mixing 40 μM recombinant Tau with 40 μM low molecular weight heparin and 2 mM DTT in 100 mM sodium acetate buffer (pH 7.0). Except 3′Myc-T40, which was agitated at 1,000 rpm for 5 days, the other proteins were incubated at 37 °C without shaking for 2–3 days. Successful fibrillization was confirmed using thioflavin T fluorescence assay, sedimentation tests, and negative stain electron microscopy (supplemental Fig. S1) as described previously (34). Before being used for transduction on cells, fibrillization mixture was centrifuged at 100,000 × g for 30 min at 4 °C. The resulting pellet was resuspended in equal volume of 100 mM sodium acetate buffer (pH 7.0), without heparin and DTT, and frozen as single use aliquots at −80 °C.

Cell Culture and Fibril Transduction—QBI-293 cells (QBiogene) were grown in full media (DMEM, 10% FBS) supplemented with penicillin/streptomycin and L-glutamine. For fibril transduction, cells were plated at 400,000/well in a 6-well tissue culture plate 1 day before transient transfection with WT or mutant Tau in pcDNA5/TO or pcDNA3.1(+) using FuGENE® 6 (Roche Applied Science) as per manufacturer's instructions at 2 μg of DNA per well. About 16 h after transfection, resuspended fibril aliquots were diluted into 10 μM using 100 mM sodium acetate buffer (pH 7.0) and sonicated with 20–30 pulses, 80 μl of which was added to one tube of BioPORTER reagent, gently vortexed for 5 s, and allowed to stand at room temperature for 5–10 min. During the formation of the pffs-reagent complex, cells were washed once with 2 ml of OptiMEM (Invitrogen) and placed on 500 μl of OptiMEM before the fibril-reagent complex was diluted with 420 μl of OptiMEM and added to cells. For experiments performed on cells plated on 12-well plates, all reagents were reduced by half. Six to seven hours after the addition of fibrils, cells were placed on starvation medium (DMEM, 0.5% FBS, penicillin/streptomycin, L-glutamine) to reduce cell division, 24 h after which they were washed once with Versene/EDTA, incubated with 0.05% trypsin/EDTA for 10 min at 37 °C to remove the majority of membrane-associated fibrils, and replated to poly-D-lysine-coated glass coverslips for immunostaining. Fixing was performed one night after replating.

For fibril alone transduction without BioPORTER reagent, cells were placed on starvation medium right before the addition of fibrils. Fibrils were processed in exactly the same way, and the same amount was used as in reagent-mediated transduction. Cells were trypsinized and replated either 4 or 30 h after the initial addition of fibrils. For experiments using WGA, different doses of WGA were added to starvation medium together with pffs. To inhibit endocytosis of WGA, 0.1 M GlcNAc was incubated with medium containing pffs and 10 μg/ml WGA for 1 h at 37 °C before being added to cells that were preincubated in 0.1 M GlcNAc-containing medium for 1 h. Cells were placed on WGA-free starvation medium 5–6 h after fibril addition and fixed after overnight incubation to minimize possible toxicity resulted from WGA treatment. No replating was done for biochemical analysis except for experiments attempting to quantify cell-associated pffs (Fig. 7*F*) and 4 h fibril-alone transduction experiments (Fig. 7*C*) in which cells were transferred to new 6-well plates after the incubation period.

Immunocytochemistry—Immunocytochemistry was performed 48 h after the initial addition of fibrils unless indicated otherwise. Cells were fixed in 4% paraformaldehyde for 10 min and permeabilized with 0.1% Triton X-100 for 15 min or fixed with 4% paraformaldehyde containing 1% Triton X-100 for 15 min to remove soluble proteins. For visualization of microtubules, cells were fixed with 0.3% glutaraldehyde in PEM buffer (80 mM PIPES (pH 6.8), 5 mM EGTA, 1 mM $MgCl_2$) for 10 min, extracted with 1% Triton X-100 for 15 min before being quenched with 10 mg/ml sodium borohydride for 7 min, followed by 0.1 M glycine for 20 min. After blocking with 3% BSA and 3% FBS for at least 1 h at room temperature, cells were incubated with specific primary antibodies (see supplemental Table 1) for 2 h at room temperature or overnight at 4 °C followed by staining with appropriate Alexa Fluor 594- or 488-conjugated secondary antibodies (goat anti-mouse/rabbit/mouse IgG1/mouse IgG2b) for 1–3 h at room temperature. DAPI was added to PBS wash to label cell nuclei. For ThS staining, cells were incubated with 0.005% ThS for 8 min and differentiated with 70% ethanol four times for 5 min each.

Two-stage immunostaining was employed to distinguish between membrane-associated and truly internalized pffs. Live cells were incubated with rabbit polyclonal anti-Myc Ab diluted in medium containing 25 mM HEPES for 1 h at 4 °C. After three washes with cold medium, cells were fixed with 4% paraformaldehyde and permeabilized with 0.1% Triton X-100. Following blocking, cells were incubated with monoclonal anti-Myc Ab 9E10 for 1–2 h at room temperature. Rabbit Myc Ab is expected to bind to cell membrane-associated pffs only, where 9E10

would bind to both membrane-associated and intracellular pffs; therefore, truly internalized pffs should only be recognized by 9E10 but not rabbit Myc Ab. Epifluorescence images were acquired using Olympus BX 51 microscope (B&B Microscopes) equipped with a digital camera DP71 (Olympus) and DP manager (Olympus).

Sequential Extraction and Western Blot—Cells were washed once with PBS before being scraped into Triton lysis buffer (1% Triton X-100 in 50 mM Tris, 150 mM NaCl (pH 7.6)) or Sarkosyl lysis buffer (1% Sarkosyl in 50 mM Tris, 150 mM NaCl (pH 7.6)) containing protease and phosphatase inhibitors and incubated on ice for 10–15 min. For Sarkosyl extraction, lysates were rotated at room temperature for 1 h before the next step. Following sonication, lysates were centrifuged at 100,000 × *g* for 30 min at 4 °C. Supernatants were kept as "Triton/Sarkosyl fraction," whereas pellets were washed once in Triton/Sarkosyl lysis buffer, resuspended, and sonicated in SDS lysis buffer (1% SDS in 50 mM Tris, 150 mM NaCl (pH 7.6)). After centrifugation at 100,000 × *g* for 30 min at 22 °C, supernatants were saved as "SDS fraction." Equal proportions of Triton/Sarkosyl and SDS fractions were resolved on 10% SDS-polyacrylamide gels, transferred to nitrocellulose membranes, and blocked in 5% milk in TBS before probing with specific Abs (see supplemental Table 1). Protein-free block (ThermoFisher) was used for PHF-1 blots.

Pulse-Chase—Reagent-mediated transduction was performed as described above. One day after transduction, cells were placed on methionine-free medium for 15 min and then pulsed with methionine-free medium containing [^{35}S]methionine (150 μCi for each well on 12-well plate) for 20 min, following which cells were switched into complete medium containing 5 mM cold methionine and chased for different durations. During harvest, cells were washed once in Hanks' balanced salt solution and sequentially extracted using 1% Triton X-100 followed by 1% SDS lysis buffer. Tau was immunoprecipitated from cell lysates using a combination of mAbs T46 and Tau 5.

Electron Microscopy (EM)—To visualize pffs made *in vitro*, 6 μl of unsonicated or sonicated fibrils was placed on 300 meshed Formvar/carbon film-coated copper grids (Electron Microscopy Sciences) for 3 min, washed twice with 50 mM Tris buffer (pH 7.6) for 5 min each, stained with 10–15 drops of 2% uranyl acetate, and visualized with Jeol 1010 transmission electron microscope (Peabody). Immuno-EM of reagent alone-treated cells and fibril-transduced cells were performed as described previously (30) using PHF-1 as the primary antibody.

Sandwich ELISA for Quantifying Acetylated Tubulin and Tau in Cell Lysates—Levels of acetylated tubulin (Ac-tub) and Tau in cell lysates were quantified using sandwich ELISA in 384-well plate format. For Ac-tub ELISA, tubulin mAb 12G10 was used as the capture antibody, and horseradish peroxidase (HRP)-conjugated Ac-tub mAb was used as the reporting antibody. Standard curves were generated using serially diluted brain lysates from WT mice. 18 μg of cell lysates diluted in EC buffer (0.02 M sodium phosphate buffer (pH 7.0), 2 mM EDTA, 0.4 M NaCl, 0.2% BSA, 0.05% CHAPS, 0.4% Blockace, 0.05% NaN_3) was loaded to each well and incubated overnight at 4 °C. The following day, after 4 h of incubation with reporting antibody at room temperature, trimethylbenzidine peroxidase substrate solution was added, and the plate was read using SpectraMax at 450 nm absorbance. For quantifying Tau in Triton and SDS fractions, cell lysates from sequential extraction were diluted 1000 times in EC buffer. Serially diluted recombinant human T40 was used to generate standard curves. 30 μl of diluted samples were loaded into each well of the plate coated with capture antibody Tau 5. After overnight incubation at 4 °C, captured proteins were reported using biotin-labeled BT2 and HT7, which were left to incubate overnight at 4 °C. The next day, following 1 h of incubation with HRP-conjugated streptavidin at 25 °C, the plate was developed using trimethylbenzidine peroxidase substrate solution.

Quantifications and Statistical Analysis—For quantifying the percentage of cells developing Tau aggregates with different combinations of endogenous Tau and pffs, 10–20 random-field images were taken at ×40 magnification for each combination, and at least two independent experiments were performed. For quantification of MT bundling and pff alone-induced Tau aggregation under various conditions (*i.e.* different temperatures, with or without WGA/GlcNAc), 10 random-field images were taken at ×20 magnification for each condition in each experiment, and 3–4 independent experiments were performed. Two-tailed paired Student's *t* test was used for all the comparisons in the study, and differences with *p* values less than 0.05 were considered significant.

RESULTS

Intracellular Tangle-like Aggregates Can Be Induced by pffs—To explore the capability of Tau pffs to seed intracellular fibrillization of soluble Tau, QBI-293 cells were transiently transfected with wild type T40 (WT-T40), the longest human Tau isoform (2N4R), and transduced with pffs generated from Myc-tagged full-length human Tau (Myc-T40) or truncated Tau containing only the four MT-binding repeats (Myc-K18) (supplemental Fig. S1) using BioPORTER protein delivery reagent. Unlike WT-T40-expressing cells treated with transduction reagent alone, in which phosphorylated Tau recognized by monoclonal antibody (mAb) PHF-1 (Ser(P)-396/404) was completely soluble and extracted by 1% Triton X-100 during fixation (Fig. 1*A*), cells transduced with either Myc-T40 or Myc-K18 Tau pffs showed accumulations of Triton-insoluble fibrillar phospho-Tau aggregates (Fig. 1*B*). These induced aggregates were also detected by anti-phospho-Tau mAb AT8 (Ser(P)-202/Thr(P)-205) and conformation-dependent mAb MC-1 (Fig. 1*C*), which specifically recognizes Tau in a pathological conformation (35). Interestingly, pff-induced aggregates exhibited a variety of morphologies, ranging from widely distributed short fibrils, skein-like accumulations, to localized dense NFT-like inclusions and sometimes a mixture of phenotypes (Fig. 1*C*).

Significantly, double labeling immunofluorescence in WT-T40-expressing cells using anti-Myc antibody to detect Myc-K18 and Myc-T40 pffs and PHF-1 to detect phosphorylated T40 showed that anti-Myc only labeled a fraction of the fibrils detected by PHF1, thus supporting a seeding and recruit-

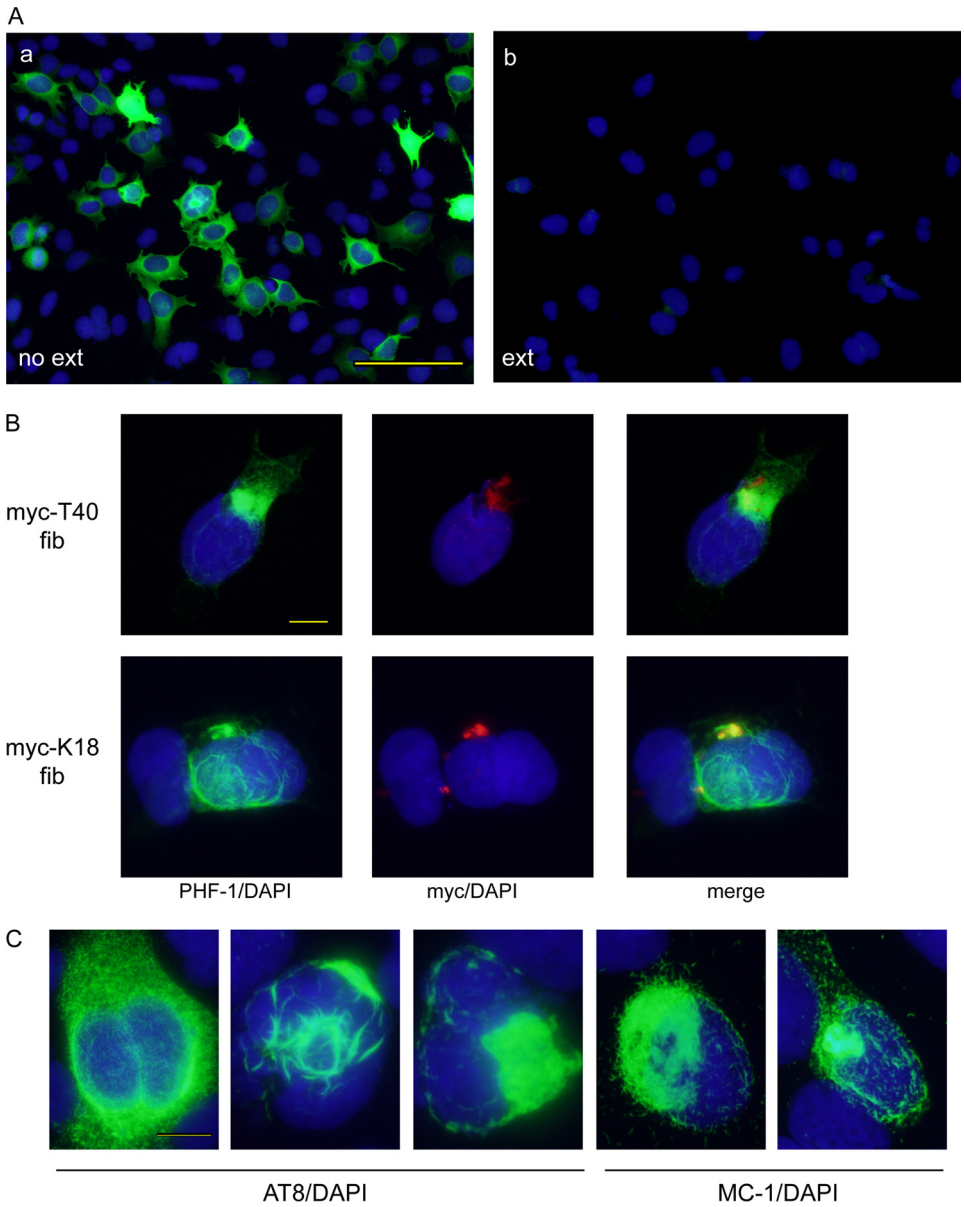

FIGURE 1. **Tau pffs seed endogenous Tau fibrillization in WT-T40-transfected QBI-293 cells.** *A,* phosphorylated Tau recognized by phospho-Tau antibody PHF-1 (*green*) was completely soluble in WT-T40-transfected cells treated with BioPORTER reagent alone. Soluble proteins were extracted (*ext*) by 1% Triton X-100 during fixing of the cells in *panel b* but not in *panel a*. *B,* intracellular accumulation of insoluble Tau recognized by PHF-1 can be induced by both Myc-T40 and Myc-K18 pffs (referred as *myc-T40 fib* and *myc-K18 fib*) transduced using BioPORTER reagent. Exogenous pffs were immunostained with polyclonal anti-Myc antibody (*red*). *C,* induced Tau aggregates showed a range of morphologies that can be recognized by phospho-Tau antibody AT8 and conformational-dependent antibody MC-1. *B* and *C,* cells were extracted with 1% Triton X-100 during fixing. In all panels, cell nuclei were stained by DAPI (*blue*). Magnification: ×20 for *A*; ×40 for *B* and *C*. *Scale bars,* 100 μm for *A*; 10 μm for *B* and *C*.

ment mechanism of Tau aggregate formation (Fig. 1*B*). Moreover, phosphorylated Tau was nonexistent or rare in non-transfected cells transduced with Myc-T40 pffs, suggesting a lack of phosphorylation of internalized full-length fibrils (data not shown). Furthermore, because epitopes recognized by these three Tau-specific mAbs (PHF-1, AT8, and MC-1) are absent from Myc-K18, their immunoreactivities in Myc-K18 fibril-transduced cells can be entirely attributed to endogenously expressed WT-T40. Thus, exogenously supplied Tau pffs do not constitute the insoluble phospho-Tau species we detect in WT-T40 cells treated with pffs. Finally, accumulation of insoluble Tau aggregates failed to occur when pffs were transduced into cells expressing fibrillization-incompetent Tau with K311D mutation (data not shown), further confirming the *de novo* fibrillization of soluble Tau in WT-T40-expressing cells.

P301L Mutation Enhances Seeded Recruitment of Endogenous Tau—To assess the efficacy of recruitment by pffs of 4R Tau, with or without N-terminal inserts, as well as disease-associated mutant Tau, fibril transduction was performed on QBI-293 cells transiently transfected with human T43 (0N4R), T40/ΔK280 (FTDP-17 mutation in the MT-binding domain), T40/P301L (FTDP-17 mutation in the MT-binding domain), and T40/R406W (FTDP-17 mutation outside the MT-binding domain). Quantification of the percentage of aggregate-bearing cells induced by these various combina-

tions revealed a similar extent of aggregation in T43- and T40-transfected cells upon Myc-K18 fibril transduction (about 8% of cells had aggregates with either treatment), suggesting the number of N-terminal inserts does not affect fibrillization (Table 1). Among the dominantly inherited Tau mutations in FTDP-17 studied here, T40 with the P301L mutation demonstrated the highest propensity of pff-induced aggregation. Specifically, transduction of Myc-K18 pffs and Myc-K18 pffs with P301L mutation (Myc-K18/P301L fibrils) led to about 20 and 35% of cells bearing aggregates, respectively (Table 1), corresponding to ~40 and ~70% of the transfected cells assuming 50% transfection efficiency (Fig. 2*A*). Although Myc-K18/P301L fibrils appeared to be better "seeds" for T40/P301L recruitment as monitored by number of aggregate-bearing cells, they were comparable with, or even slightly less efficient than, Myc-K18 fibrils in nucleating the fibrillization of WT-T40 (Table 1). Enhanced aggregation of T40/P301L as compared with WT-T40 corresponded to significantly more accumulation of Triton-insoluble Tau as shown on immunoblots (compare Fig. 2*B* with supplemental Fig. S2*B*). The induced Tau aggregates were also Sarkosyl-insoluble, with the immunoblot of Sarkosyl extraction indistinguishable from that of Triton extraction (supplemental Fig. S3).

Quantification by Tau sandwich ELISA indicated that Myc-K18/P301L pffs always resulted in higher amounts of Triton-insoluble T40/P301L Tau than Myc-K18 pffs, confirming a more efficient recruitment of soluble Tau with the combination of Myc-K18/P301L pffs and T40/P301L-expressing cells (Fig. 2*C*). Interestingly, both Myc-K18 and Myc-K18/P301L pff transduction on T40/P301L-expressing cells invariably led to a reduction of Triton-soluble Tau when compared with non-transduced cells, further supporting that the accumulation of insoluble Tau is through sequestration/recruitment of soluble Tau.

Intriguingly, live immunostaining followed by immunofluorescence after fixation and permeabilization (two-stage staining) revealed that the majority of pffs associated with cells were merely membrane-associated despite extensive trypsinization before replating cells to coverslips, and only a small amount of pffs were truly internalized (Fig. 3*A*). Moreover, double labeling using anti-Myc antibody and PHF-1 in cells extracted with 1% Triton X-100 showed that less than half of the induced aggregates contained detectable colocalizing pffs (Fig. 3*B*), suggesting that small amounts of pff

TABLE 1

% of aggregate-bearing cells with specific combinations of endogenous Tau transfection and fibril transduction

Fibrils	Transfection				
	WTT40 (2N4R)	T43 (0N4R)	T40/ P301L	T40/ ΔK280	T40/ R406W
			%		
5′myc-K18	~8	~8	~20	~5	~6
5′myc-K18/P301L	~5	NT[a]	~35	NT	NT

[a] NT means not tested.

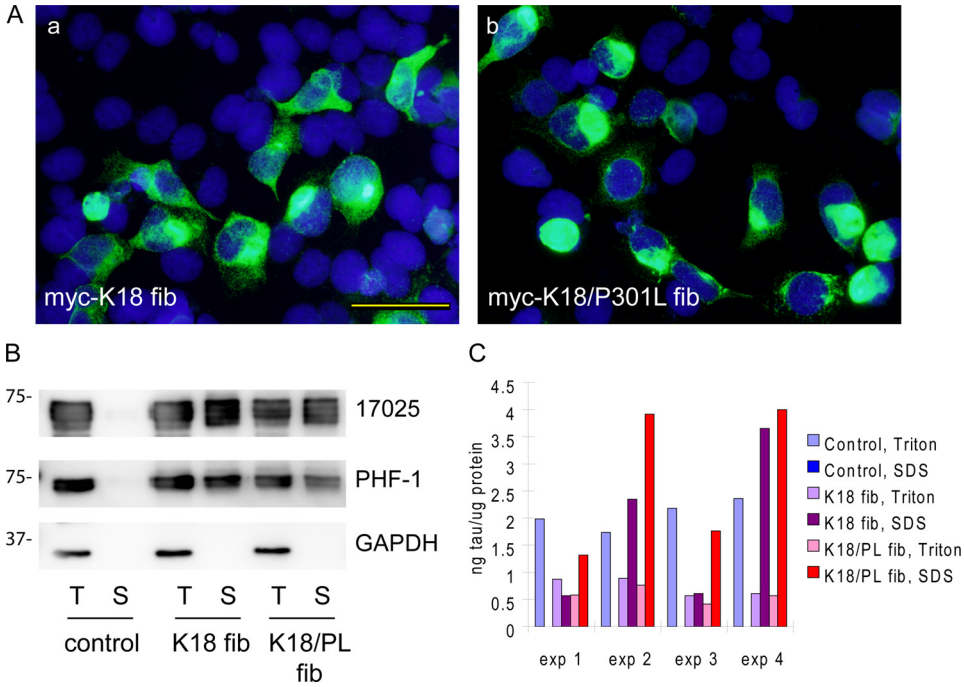

FIGURE 2. **P301L mutation enhances pff-induced aggregation.** *A*, QBI-293 cells were transiently transfected with T40 with P301L mutation (T40/P301L) and transduced with Myc-K18 fibrils (*fib*) (*panel a*) or Myc-K18/P301L fibrils (*panel b*) using BioPORTER reagent. Abundant Tau aggregates were detected using mAb PHF-1 (*green*) after simultaneous 1% Triton X-100 extraction during fixation to remove soluble proteins. *B*, sequential extraction was performed on T40/P301L-transfected cells treated with BioPORTER reagent alone (control), with Myc-K18 fibrils (*K18 fib*), or Myc-K18/P301L fibrils (*K18/PL fib*). *T* indicates the cellular fraction recovered in 1% Triton X-100 lysis buffer. *S* indicates the Triton-insoluble fraction solubilized in 1% SDS lysis buffer. Equal proportions of Triton and SDS fractions were loaded on SDS-polyacrylamide gels. Immunoblotting with polyclonal Tau Ab 17025 and PHF-1 revealed accumulation of abundant Triton-insoluble Tau in fibril transduced cells. GAPDH served as a loading control. *C*, sandwich Tau ELISA on cell lysates from four independent experiments (*exp*) confirmed induction of significant amount of Triton-insoluble Tau with fibril transduction, which was always accompanied by a reduction in soluble Tau. Magnification: ×40. *Scale bar*, 50 μm.

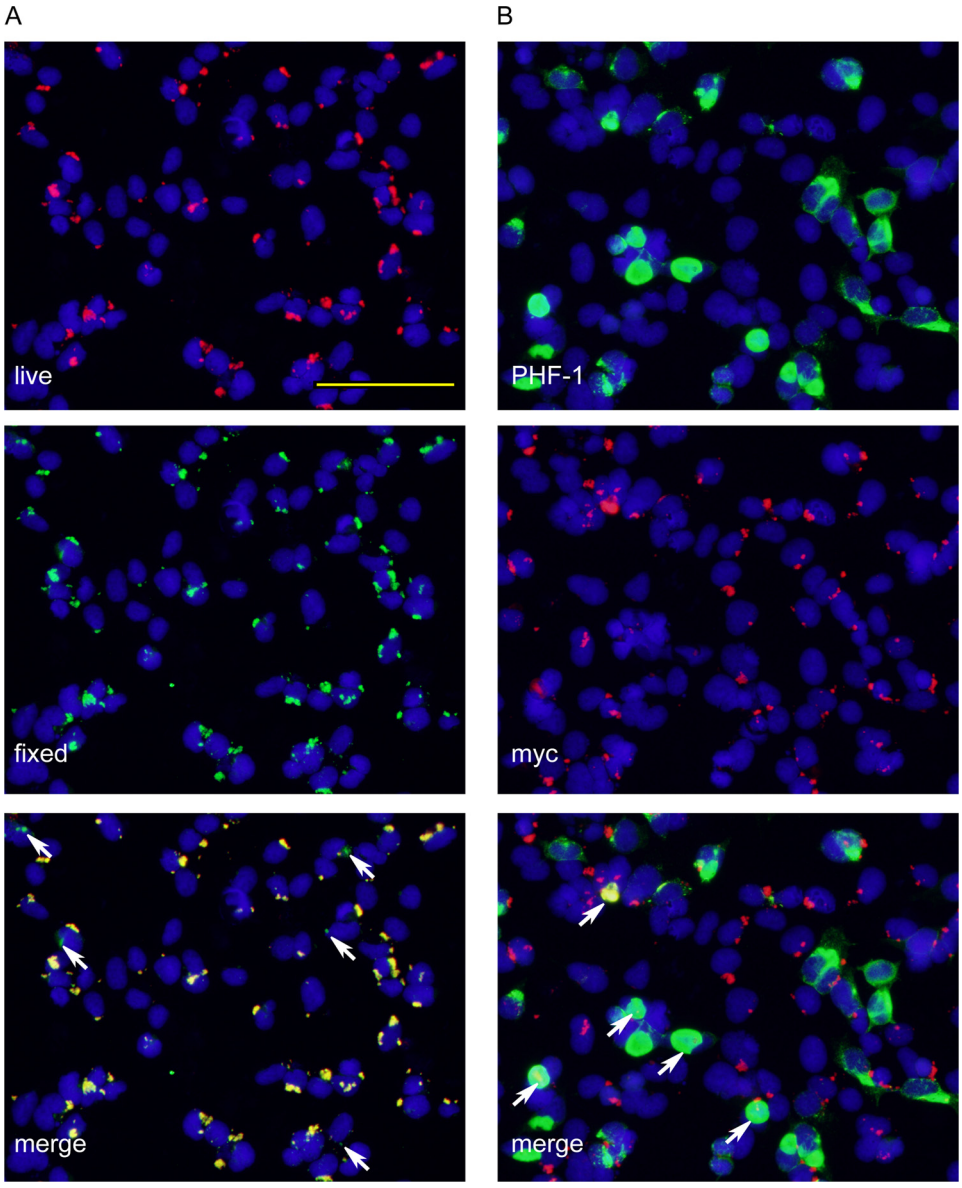

FIGURE 3. **Internalization of small quantities of Tau pffs is sufficient to induce robust Tau aggregation.** QBI-293 cells were transiently transfected with mutant T40/P301L Tau and transduced with Myc-K18/P301L pffs using BioPORTER reagent. *A,* incubation of fibril-transduced cells with polyclonal anti-Myc antibody before fixing (live, *red*) followed by staining of fixed and permeabilized cells with anti-Myc mAb 9E10 (fixed, *green*) showed extensive colocalization, suggesting the majority of the pffs detected were merely extracellularly associated with cell membranes. *Arrows* point to truly internalized fibrils that were only recognized by 9E10 applied to fixed and permeabilized cells but not polyclonal anti-Myc antibody used on live cells. *B,* double labeling of phospho-aggregates by PHF-1 (*green*) and exogenous pffs by polyclonal anti-Myc (*red*) showed very little colocalization. *Arrows* point to aggregates with colocalizing pff seeds. Aggregates without *arrows* do not contain obvious pff seeds. Magnification: ×20. *Scale bar,* 100 μm.

seeds are sufficient to induce robust endogenous Tau fibrillization.

pff-induced Tau Aggregates Are Composed of Filamentous NFT-like Amyloid Structures—Routine EM and immuno-EM using PHF-1 revealed abundant cytoplasmic filaments in pff-transduced cells (Fig. 4) but not in those treated with transduction reagent alone. Moreover, diverse organelles, including mitochondria, lysosomes, and other vesicular structures, were detected within and adjacent to PHF-1-positive filamentous structures (Fig. 4*A*, *panels a* and *b*). The lack of diffuse PHF-1 staining in the cytoplasm outside of the PHF inclusions further supports the concept of seeding and recruitment of soluble Tau to form NFT-like structures in pff-transduced cells.

To examine the progression of pff-induced endogenous Tau aggregation, we fixed cells at different time points after the addition of the pff-reagent complex. At $t = 1$ h, there was little accumulation of Triton-insoluble Tau, except for a few rare cells showing focal PHF-1 immunoreactivities with small but intensely labeled inclusions surrounded by slender, discrete fibrillar structures (supplemental Fig. S4*A*). At $t = 3$ h, focal inclusions became more frequent, and a small population of cells developed skein-like accumulations throughout the cytoplasm (Fig. 5*A*). It is noteworthy that the earliest focal accumulations were almost always colocalized with Myc immunoreactivities, suggesting that aggregation first begins in cells containing more abundant fibril seeds that rapidly initiate the

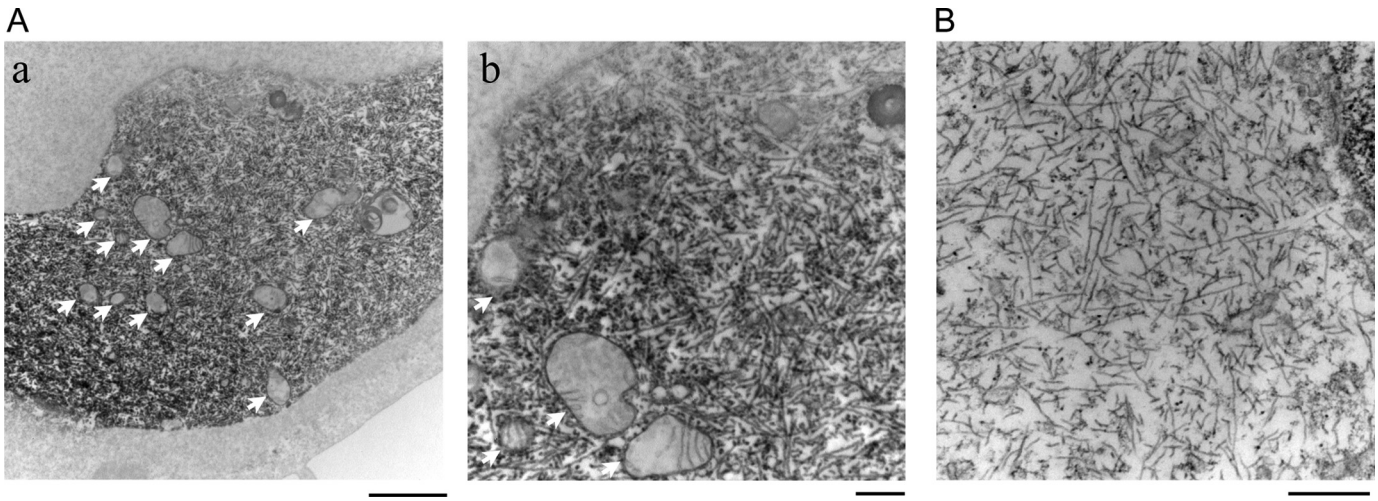

FIGURE 4. **pff-induced Tau aggregates consist of filamentous structures.** T40/P301L-transfected QBI-293 cells were transduced with Myc-K18/P301L fibrils using BioPORTER reagent. *A,* immuno-EM using mAb PHF-1 showed abundant filamentous Tau aggregates in the cytoplasm. *Arrows* indicate mitochondria and/or vesicular structures in close association with Tau fibrils. *B,* routine EM showing pff-induced Tau fibrils. Magnification: ×12,000 for *A, panel a*; ×30,000 for *A, panel b*; 50,000 for *B*. *Scale bars*: 2 μm for *A, panel a*; 500 nm for *A, panel b,* and *B*.

conversion of endogenous Tau into insoluble aggregates through physical recruitment. At $t = 6$ h, insoluble Tau was found in about 4% of total cells. Although diffuse fibrillar accumulations remained the most common phenotype at this stage, some aggregates started showing signs of coalescence, and large compact inclusions appeared in a small subset of cells (Fig. 5*B*). Twenty four hours after fibril transduction, about 25% of total cells were replete with Triton-insoluble Tau, with a significant portion of cells bearing large, densely packed aggregates (Fig. 5*C*). ThS was used to determine whether pff-induced Tau aggregates form amyloid fibrils. Up to $t = 3$ h, ThS staining completely overlapped the Myc immunoreactivities, indicating exclusive recognition of β-pleated sheet in Myc-K18/P301L pffs (supplemental Fig. S4*B*). ThS staining that colocalized with PHF-1-positive endogenous Tau aggregates first emerged at $t = 6$ h and became more abundant at $t = 24$ h (Fig. 5, *B* and *C*). Interestingly, only the large compact aggregates, but not diffuse skein-like inclusions, were recognized by ThS. We speculate that dispersed fibrillar aggregates probably represent early fibril species that eventually coalesce and mature into β-sheet-rich inclusions.

Newly Synthesized Tau Is Recruited Rapidly into Insoluble Tau Fibrils—To directly monitor the recruitment of newly synthesized Tau into insoluble aggregates, we performed pulse-chase experiments on Myc-K18/P301L pff-transduced T40/P301L-expressing cells. In cells treated with transduction reagent alone, ^{35}S-radiolabeled Tau remained soluble over a 6-h chase period despite a time-dependent electrophoretic mobility shift indicative of phosphorylation of the newly synthesized Tau. In contrast, an increasing proportion of radiolabeled T40/P301L Tau emerged in the Triton-insoluble fraction of fibril-transduced cells, accompanied by more rapid reduction of soluble Tau than in the control cells, demonstrating active recruitment of newly synthesized Tau into an insoluble pool (Fig. 6). After a 1-h chase, an appreciable amount of T40/P301L Tau was already detected in the insoluble fraction, highlighting the rapid solubility change of Tau in the presence of misfolded seeds. Moreover, the detection of slower migrating insoluble radiolabeled Tau suggests continuous recruitment of soluble Tau that is being modified by phosphorylation over time.

Reduced MT Stability Is Associated with Tau Aggregation—Consistent with previous studies in other cell lines, overexpression of Tau in QBI-293 cells led to the formation of thick MT bundles due to excessive stabilization of MTs (21, 36). We hypothesized that seeded recruitment of Tau into insoluble fibrils may attenuate the overstabilization of MTs by sequestering the soluble pool of Tau. As expected, T40/P301L-expressing cells that were transduced with Myc-K18 or Myc-K18/P301L pffs showed significantly less MT bundling revealed by immunostaining of Ac-tub, a marker of stable MTs, as compared with those treated with transduction reagent alone (~40 and ~60% reduction in the percentage of cells with MT bundles by Myc-K18 and Myc-K18/P301L pff transduction, respectively) (Fig. 7, *A* and *C*). The majority of cells with aggregates showed an absence of MT bundles, and cells that retained bundles typically showed diffuse Tau staining (Fig. 7*B*). Reduced Ac-tub levels associated with pff-induced aggregation was further confirmed using an Ac-tub sandwich ELISA (Fig. 7*D*). In addition, there was a significant correlation between Ac-tub level and soluble Tau, but not insoluble Tau, suggesting that the loss of soluble Tau rather then aggregation *per se* was responsible for the reduced MT stability (Fig. 7, *E* and *F*). This observation likely accounts for the occasional MT bundles observed in cells carrying aggregates (data not shown).

Spontaneous Fibril Uptake Is Mediated by Endocytosis—To determine whether Tau pffs can be taken up spontaneously in the absence of protein delivery reagent, we incubated T40/P301L-transfected cells with Myc-K18/P301L pffs for 30 h, followed by trypsinization and incubation for an additional 18 h. Aggregation of endogenous Tau was detected in about 10% of total cells, accompanied by appreciable accumulation of Triton-insoluble Tau detected on immunoblots (Fig. 8, *A, panel a,* and *B*). Interestingly, exogenous pffs were barely visible by immunostaining (Fig. 8*E*), suggesting that inter-

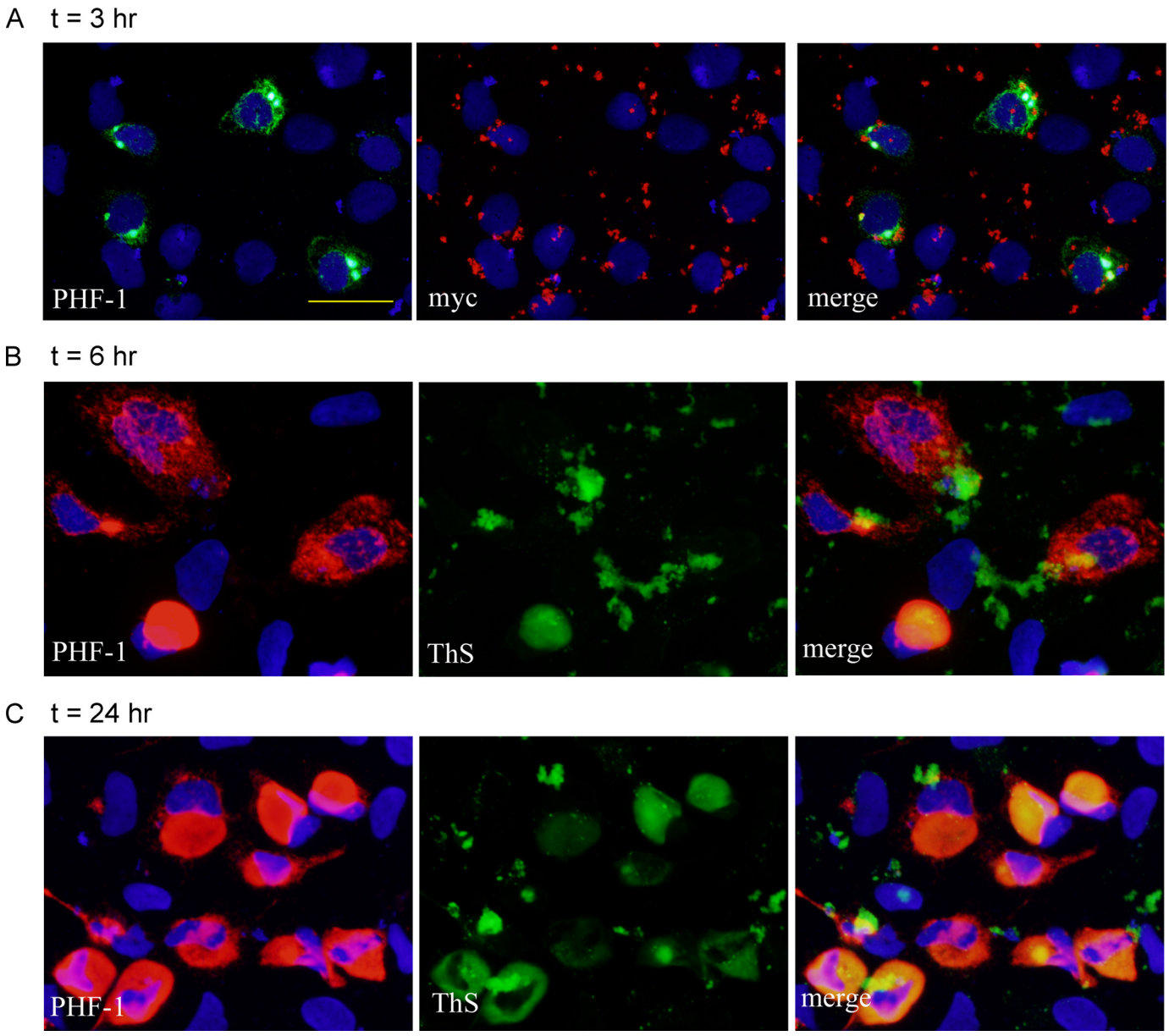

FIGURE 5. **Time-dependent development of insoluble Tau aggregates.** QBI-293 cells transfected with T40/P301L mutant Tau were transduced with Myc-K18/P301L fibrils using BioPORTER reagent. *A,* at $t = 3$ h after the addition of fibril-reagent complex, a small percentage of cells started showing accumulations of insoluble Tau (PHF-1) with focal inclusions colocalizing with pff staining (*myc*). *B,* at $t = 6$ h, more cells developed aggregates, most of which are skein-like and diffusely distributed throughout the cytoplasm. A small population of cells showed ThS-positive large aggregates. *C,* large aggregates recognized by ThS were more frequently seen at $t = 24$ h after fibril addition. Soluble proteins were extracted by 1% Triton X-100 during fixing for all. Magnification: ×40. *Scale bar,* 50 μm.

nalization of minute quantities of pffs without transduction reagent is sufficient to induce recruitment of endogenous Tau into fibrils. To investigate whether this uptake of Tau pffs occurs by endocytosis, we incubated T40/P301L-expressing cells with Myc-K18/P301L pffs for 4 h at either 37 °C or 4 °C; the latter temperature blocks endocytosis. Because the amount of pff internalized by cells is too low to be easily detected by either immunostaining or immunoblotting (Fig. 8, *E* and *F*), we quantified Triton-insoluble endogenous Tau aggregates as an indirect readout of pff entry. Pff incubation at 37 °C for 4 h prior to trypsinization and an additional 44-h incubation resulted in ~3% of total cells with Tau inclusions, whereas 4 h of pff incubation at 4 °C followed by exactly the same treatments resulted in a dramatic and significant reduction in the percentage of Tau aggregate-bearing cells (Fig. 8, *A*, *C* and *D*), suggesting pff uptake is a temperature-dependent process. The small number of cells with Tau aggregates (~0.5% of total cells) detected after 4 °C of pff incubation could be due to the internalization of residual membrane-associated fibrils following trypsinization and additional incubation. Moreover, the difference in the extent of aggregation induced by 4 *versus* 30 h of incubation of pffs (~3% *versus* ~10% aggregate-bearing cells) indicated a time-dependent internalization of fibrils (Fig. 8*D*). These results suggest spontaneous uptake of pffs probably occurs by endocytosis.

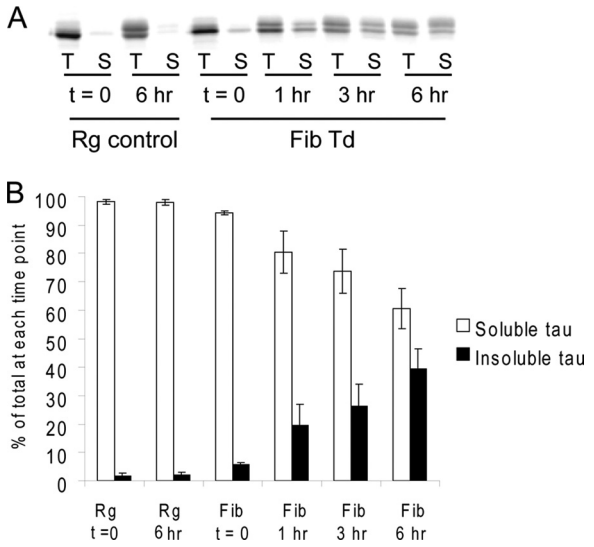

FIGURE 6. **Newly synthesized Tau is rapidly recruited into insoluble aggregates.** One day after Myc-K18/P301L fibril transduction on QBI-293 cells transiently transfected with T40/P301L, cells were pulsed with [^{35}S]methionine for 20 min and chased for different durations (0–6 h). Cell lysates were sequentially extracted using 1% Triton X-100 followed by 1% SDS lysis buffer, and Tau was immunoprecipitated from both fractions with mAbs T46 and Tau 5. Equal proportions of Triton (*T*) and SDS (*S*) fractions were loaded on SDS-PAGE for autoradiography. *A,* autoradiograph indicating that newly synthesized Tau remained soluble in cells treated with reagent alone (*Rg control*) but rapidly turned insoluble in fibril-transduced cells (*Fib Td*). *B,* quantification from two independent experiments showing the distribution of radiolabeled Tau in the soluble and insoluble fractions over time (*error bar,* standard error).

Adsorptive Endocytosis Enhances Tau pff Uptake—To further explore potential mechanisms of endocytosis-mediated pff entry, we incubated cells with pffs in the presence of WGA, a plant lectin that has high affinity for GlcNAc and sialic acid on the plasma membrane and is readily internalized by cells via adsorptive endocytosis (37, 38). Apart from being a substrate of the endocytic pathway, WGA was also shown to potentiate the uptake of other proteins mediated by the same endocytic pathway (39, 40). Interestingly, we found that WGA increased the prevalence of Tau aggregate-bearing cells (Fig. 9, *A* and *B*) and the amount of Triton-insoluble Tau in fibril-transduced cells (Fig. 9*C*) in a dose-dependent manner, which paralleled increased cellular association with pffs (Fig. 9*D*). Without WGA treatment, there was minimal fibril staining even without trypsinization. Increasing the dose of WGA not only led to progressively more abundant cell-associated pffs, but two-stage staining revealed that a substantial percentage of these fibrils was indeed intracellular (Fig. 9*E*). Furthermore, the effects of WGA on pff uptake and Tau aggregation were significantly attenuated by adding 0.1 M GlcNAc to the medium, which reduces WGA-plasma membrane interactions through competition with GlcNAc on the plasma membrane (37), suggesting that WGA-mediated induction of adsorptive endocytosis is necessary for increased pff uptake and augmented Tau aggregation (supplemental Fig. S5*B* and Fig. 9, *F* and *G*). On the other hand, up to 15 μg/ml of WGA does not increase the expression level of Tau nor does it induce accumulation of insoluble Tau in the absence of pffs (supplemental Fig. S5*A*). Therefore, increased intracellular Tau aggregate formation by WGA treatment is primarily due to enhanced internalization of pffs. Taken together, spontaneous pff entry seems to occur at least in part through adsorptive endocytosis, which can be potentiated by WGA.

DISCUSSION

Our study convincingly demonstrates that exogenously supplied Tau pff seeds can recruit soluble endogenous Tau into insoluble fibrillar aggregates that highly resemble NFTs based on a variety of criteria, including immunofluorescence, amyloid dye binding, immuno-EM, and biochemical analysis. Interestingly, a small quantity of internalized Tau pffs appears sufficient to recruit and sequester large amounts of endogenous Tau into filamentous Tau inclusions. Sequestration of soluble Tau by pff-induced aggregation significantly attenuates MT overstabilization resulting from Tau overexpression, supporting the concept that there is a reduction of soluble Tau in neurodegenerative tauopathies. Intriguingly, substantial aggregation of soluble Tau can also be induced by the spontaneous uptake of pffs, which seems to occur via adsorptive endocytosis that is potentiated by the plant lectin WGA, demonstrating a cellular transmissibility of Tau pathology.

Although the uptake and seeding capacity of preformed Tau fibrils in cultured cells was reported recently (29, 31), the induction and formation of intracellular aggregates in this study are fundamentally different from those previous studies in several ways. First, the intracellular aggregates induced in our model are morphologically different from previous studies. The inclusions we observed are clearly fibrillar in nature and mature into β-pleated sheet-rich fibrils recognized by ThS. Second, similar to Tau tangles detected in AD and other tauopathies, the intracellular aggregates exhibit a diversity of morphologies, ranging from spatially distributed skein-like accumulations to large and densely packed aggregates, which probably represent different stages of aggregation. Third, unlike previous reports, detectable pff seeds rarely coincide with the intracellular inclusions in our system; instead, the majority of aggregates that are composed of recruited, phosphorylated endogenous Tau greatly exceed the physical size of the seeds. Fourth, our use of protein delivery reagents to augment introduction of pffs into cells provides better efficiency of Tau pff entry as compared with previous reports. Finally, unlike previous studies that expressed endogenous Tau tagged with a fluorescent protein, our system employs untagged Tau that facilitates recruitment because the large fluorescent protein tag may interfere with the conformational change required for efficient Tau fibril assembly.

For the past 20 years, significant efforts have been devoted to produce cell-based models that develop Tau aggregates similar to those observed in tauopathies but with little success. This is because Tau is a highly soluble and naturally unfolded protein, and therefore, it has been notoriously difficult to make it aggregate in cultured cells. Strategies have been used in the past with minimal success to produce Tau tangles in cells, including overexpression of aggregation-prone Tau mutants (22), overexpression of truncated Tau that fibrillizes more readily than full-length Tau (41, 42), addition of pre-aggregated amyloid-β

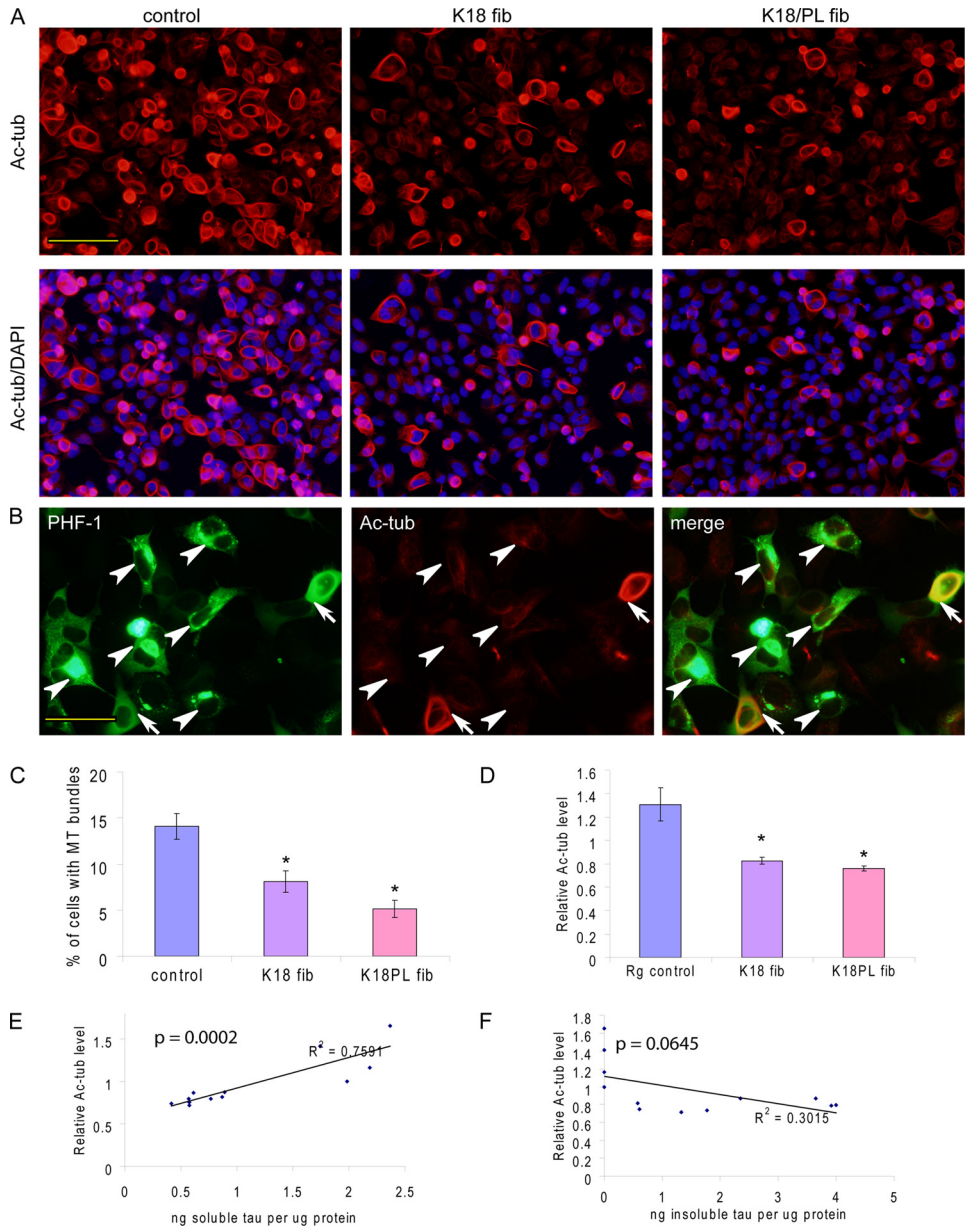

FIGURE 7. **Tau aggregation results in reduced MT stability.** *A,* QBI-293 cells transfected with T40/P301L and transduced with Myc-K18 (*K18 fib*) or Myc-K18/P301L (*K18/PL fib*) pffs showed significant reductions in MT bundling compared with control cells treated with BioPORTER transduction reagent alone (control), as revealed by acetylated tubulin (*Ac-tub*) staining. *B,* double staining of PHF-1 and Ac-tub showed that cells with MT bundles usually showed diffuse Tau immunostaining (*arrows*), whereas those with Tau aggregates often lacked bundling (*arrowheads*). *C,* quantification from three independent experiments demonstrated statistically significant reduction in the percentage of cells with MT bundles in the presence of fibril transduction (*error bar,* standard error; *, $p < 0.05$). *D,* Ac-tub sandwich ELISA on samples from four independent experiments showed significant decrease in Ac-tub levels associated with fibril transduction (*error bar,* standard error; *, $p < 0.05$). *E* and *F,* Ac-tub and Tau sandwich ELISA revealed highly significant correlation of Ac-tub levels with Triton-soluble Tau (*E*, $p < 0.0005$), but not with Triton-insoluble Tau (*F*, $p > 0.05$), across control and fibril-transduced samples from four independent experiments. Magnification: ×20 for *A*; ×40 for *B*. *Scale bar,* 100 μm for *A*; 50 μm for *B*.

fibrils (43), treatment conditions that promote Tau phosphorylation (44), and the addition of aromatic dyes such as Congo Red to overcome the kinetic barrier of fibrillization (45). In our optimized system, however, Tau aggregation could be rapidly induced within hours after the introduction of small quantities of misfolded Tau pffs and result in the accumulation of large amounts of insoluble Tau fibrils. Thus, such robust induction of authentic NFT-like accumulations suggests that a seeding-recruitment process is a highly plausible mechanism underlying NFT formation *in vivo* in the absence of Tau overexpression. Conceivably, pff-induced aggregation that occurs within hours/days in Tau-overexpressing cultured cells could be prolonged into a pathological event that happens over years or even decades under physiological conditions, *i.e.* in human brains. Although our time course experiments, which reveal close association of pff seeds with endogenous phosphorylated Tau aggregates at early time points, suggest a direct physical recruitment of soluble endogenous Tau by exogenous pffs to account for the solubility change of the former, we do not rule out possible conformational changes of soluble Tau templated by misfolded seeds before it elongates onto the existing intracellular fibrils.

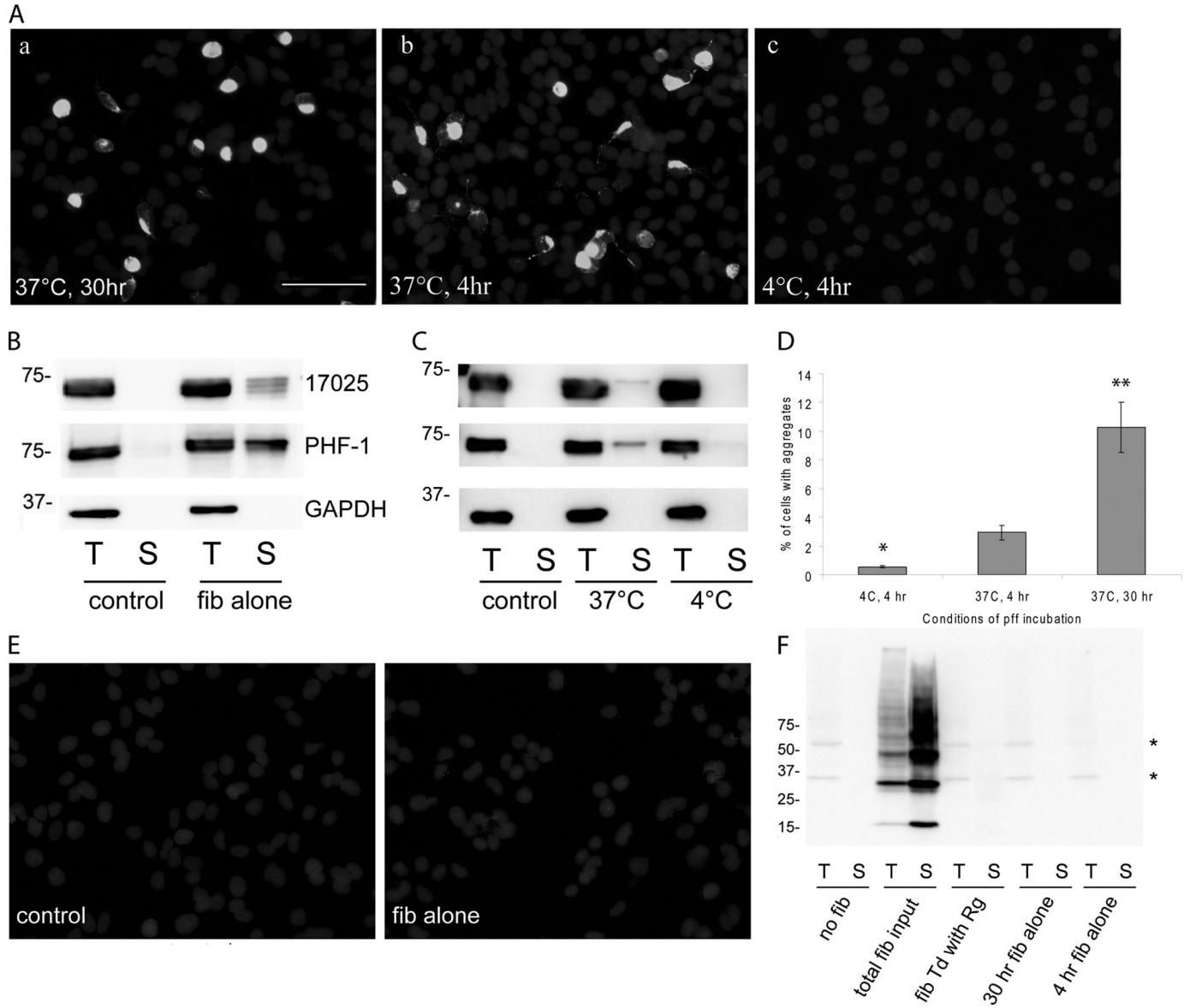

FIGURE 8. **Spontaneous uptake of pffs without transduction reagent also induces intracellular Tau aggregation.** *A,* T40/P301L aggregation induced by Myc-K18/P301L pffs alone after 30 h of incubation at 37 °C (*panel a*) or 4 h incubation at 37 °C (*panel b*). Minimal aggregation was observed with 4 h of incubation at 4 °C (*panel c*). For all conditions, cells were trypsinized and replated after the designated incubation period and fixed 48 h after the initial addition of fibrils. Soluble proteins were extracted with 1% Triton X-100 during fixing. *White,* PHF-1. *B,* 48 h incubation with Myc-K18/P301L pffs at 37 °C led to significant accumulation of Triton-insoluble T40/P301L detected on immunoblots. Control cells were transfected with T40/P301L without fibril transduction. *C,* 4 h of incubation with Myc-K18/P301L fibrils at 37 °C but not at 4 °C resulted in detectable T40/P301L Triton-insoluble aggregates. *D,* quantification from four independent experiments showed significant reduction in aggregate-bearing cells when a 4-h fibril incubation was performed at 4 °C instead of 37 °C (*error bar,* standard error; *, $p < 0.05$ compared with 4 h of incubation at 37 °C). Thirty-hour incubation with Tau pffs at 37 °C resulted in the highest incidence of aggregates ($n = 3$; *error bar,* standard error; **, $p < 0.01$ compared with 4 h incubation at 37 °C). *E,* Myc-tagged pffs were barely visible in cells transduced with fibrils (*fib*) alone without BioPORTER reagent. *White,* anti-Myc Ab. *F,* exogenous Myc-tagged Tau pffs were nondetectable with anti-Myc mAb 9E10 via immunoblot under various transduction paradigms: transduction of pffs with BioPORTER reagent (*fib Td with Rg*), 30 h of incubation with pffs alone (*30* h *fib alone*), or 4 h incubation with fibrils alone (*4 h fib alone*). Cells were trypsinized and replated to new wells after the designated incubation time so that the majority of extracellularly associated pffs were removed. *Total fib input*, amount of Tau pffs used for transduction was added to cells immediately before lysing. *, nonspecific bands. *B, C,* and *F, T* indicates 1% Triton X-100 fraction; *S* indicates 1% SDS fraction. Equal proportions of Triton and SDS fractions were loaded on SDS-polyacrylamide gels. Magnification: ×20. *Scale bar,* 100 μm.

Our studies also demonstrate that the formation of intracellular Tau tangles can be accelerated by FTDP-17 genetic mutations that were shown previously to increase the fibrillization propensity and/or reduce the MT-binding affinity of Tau (46–49). Among the FTDP-17 associated mutations (ΔK280, P301L, and R406W) tested in our model, only P301L, the most aggressive disease causing mutation found in FTDP-17 patients, dramatically promoted aggregation. This correlates well with the rapid clinical onset and progression observed in FTDP-17 patients (50–52) and transgenic mice harboring P301L mutant Tau (53–55). However, unlike a previous study that was unable to demonstrate recombinant P301L mutant Tau seeding WT Tau in a cell-free system (56), we found that WT and P301L mutant Tau can cross-seed each other readily, although fibril seeds composed of P301L mutant are slightly less efficient in recruiting WT-T40 than WT seeds. In addition, the difference

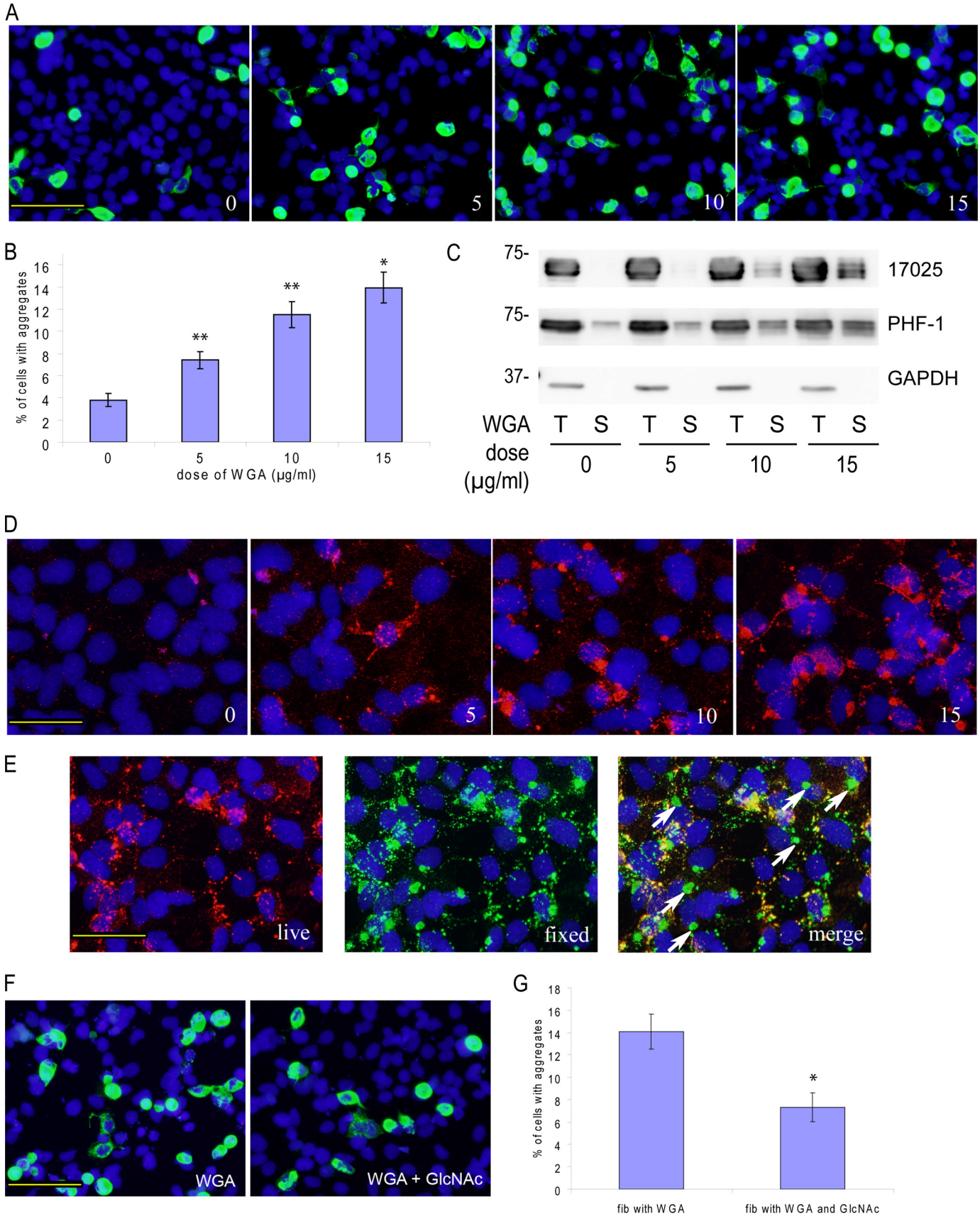
A
0
5
10
15
B
% of cells with aggregates
dose of WGA (μg/ml)
C
75-
75-
37-
17025
PHF-1
GAPDH
WGA dose (μg/ml)
T S T S T S T S
0 5 10 15
D
E
live
fixed
merge
F
WGA
WGA + GlcNAc
G
% of cells with aggregates
fib with WGA
fib with WGA and GlcNAc

in aggregation propensity between WT Tau and P301L Tau observed in our cellular model may be further magnified in a physiological setting where Tau is not overexpressed. This may explain the absence of insoluble WT Tau deposition in FTDP-17 patients with P301L mutation (57), where the overwhelmingly higher fibrillization propensity of P301L mutant Tau could mask the much slower aggregation of WT Tau that may not occur to an appreciable extent during a short disease course.

Despite lower MT-binding affinity of T40/P301L compared with WT-T40, QBI-293 cells transiently overexpressing T40/P301L mutant Tau are still capable of MT bundling. Interestingly, pff-induced aggregation resulted in significant attenuation of this phenotype. Reduced stable MTs is a well established feature of tauopathy brains (58–60), but studies exploring the relationship between compromised MT stability and Tau aggregation were based on postmortem brain examination and therefore are only correlative. Our study demonstrates a direct causal link between Tau aggregation and reduced MT stability, although we showed earlier that MT stability is reduced following phosphatase inhibitor treatment of cultured neurons, which increases Tau phosphorylation (61). Thus, both Tau aggregation and hyperphosphorylation could act synergistically to reduce MT stability. Significantly, we observed a strong correlation between MT stability and the amount of soluble Tau, but not insoluble Tau, suggesting depletion of soluble Tau into fibrillar aggregates rather than aggregates themselves is responsible for a diminution of stable MTs. Although our observations were made in an artificial cell system with overexpression of Tau, it is highly plausible that tangle formation in human brains, where the majority of Tau is normally bound to MTs for maintaining their stability, could impair the integrity of MTs by a similar mechanism of soluble Tau sequestration. Given the critical role of MTs in axonal transport and consequently neuronal survival, our study supports the loss-of-function hypothesis of NFT toxicity. Consistent with this interpretation are studies demonstrating the beneficial effects of MT-stabilizing drugs in mouse models of tauopathy without direct modulation of Tau aggregation (62, 63).

Although our study did not address the origination of misfolded seeds *in vivo*, we discovered that the amount of internalized pffs required for robust aggregation to occur was surprisingly small and barely detectable in our system. This finding holds important implications for tauopathies: it is conceivable that a small amount of misfolded seeds of Tau slowly accumulated over decades in post-mitotic neurons can eventually initiate a full blown cascade of massive aggregation of soluble Tau, rendering tangle formation a self-perpetuating event once initiated. The sonicated pffs we introduced into cells contain a heterogeneous mixture of fibrillar species with varying dimensions, and intracellular aggregates that formed without coincident detectable pffs were likely seeded by species that were too small to be visualized by light microscopy. Further studies are required to characterize the exact biophysical properties of the seeding species and to explore possible mechanisms underlying the formation of recruitment-competent aggregation seeds *in vivo*.

Consistent with recent studies pointing to the possible transmissibility of disease-associated amyloidogenic proteins (reviewed in Refs. 64, 65), we found that Tau pffs alone can also induce formation of tangle-like accumulations in a substantial population of cells, albeit to a lower extent than in the presence of protein delivery reagent. Our study thus complements an earlier *in vivo* study on the transmission of Tau pathology in mouse brains (32) by implicating Tau fibrils present in the brain extracts as the entity solely responsible for the induction and spreading of Tau pathology. Moreover, faster induction of Tau aggregation and easier manipulation of our cell culture model than animal models allow us to conduct mechanistic studies that cannot be accomplished *in vivo*. In fact, we discovered from our cellular system that spontaneous uptake of Tau fibrils appears to occur via endocytic pathways that are temperature- and time-dependent, and the potentiation of Tau aggregate formation by WGA treatment suggests that fibril entry is probably mediated, at least partly, by adsorptive endocytosis. This indicates a potential mechanism through which aggregated Tau released from dying/dead neurons or from extracellular "ghost tangles" may gain access into surrounding healthy neurons where it nucleates fibrillization of soluble Tau. Taken together, our study provides further evidence for the "prion-like" properties of Tau and offers plausible explanation for the stereotypical propagation of Tau pathology in AD brains (66) and the successful application of immunotherapy in ameliorating Tau pathology in a mouse model (67). Further studies are needed to investigate whether misfolded Tau can also be routinely secreted into the extracellular space, which would provide additional insight into the transmission cycle of Tau lesions.

In summary, we have established a simple and yet highly reproducible and robust cellular system of Tau aggregation recapitulating key features of tauopathies. We have employed this system to gain important insights into the onset and progression of Tau pathology. Our cell-based tauopathy model not only provides an invaluable tool for studying the pathogenesis of Tau aggregation, but it also offers a potential system for

FIGURE 9. **WGA promotes pff-induced Tau aggregation by enhancing spontaneous pff uptake.** *A,* T40/P301L-transfected cells were incubated with Myc-K18/P301L pffs in the presence of 0, 5, 10, and 15 μg/ml of WGA (0, 5, 10, and 15) without BioPORTER reagent. Increasing doses of WGA resulted in more frequent phospho-Tau aggregates. *Green,* PHF-1 with 1% Triton X-100 added during fixing of the cells. *B,* quantification from three independent experiments indicated that WGA dose-dependently increased the percentage of cells with aggregation (*error bar,* standard error; *, $p < 0.05$; **, $p < 0.01$). *C,* WGA treatment increased accumulation of Triton-insoluble Tau shown on immunoblots. *T* indicates 1% Triton X-100 fraction; *S* indicates 1% SDS fraction. Equal proportions of Triton X-100 and SDS fractions were loaded on SDS-PAGE. *D,* WGA also dose-dependently (0, 5, 10, and 15 μg/ml) increased the amount of cell-associated pffs revealed by Myc immunoreactivities (*red*). *E,* two-stage immunostaining (see "Experimental Procedures") performed on cells treated with 15 μg/ml of WGA showed frequent occurrence of truly internalized pffs that were only labeled by 9E10 (*green, fixed*) applied to fixed and permeabilized cells but not polyclonal anti-Myc antibody incubated with live cells (*red, live*). *Arrows* point to examples of truly intracellular pffs. *F,* GlcNAc, which inhibits binding of WGA to plasma membrane, dramatically attenuated the aggregation-enhancing effects of WGA. *G,* quantification from three independent experiments showed significant reduction of Tau aggregation in WGA-treated fibril transduced cells in the presence of GlcNAc (*error bar,* standard error; *, $p < 0.05$). Magnification: ×20 in *A* and *F*; ×40 in *D* and *E*. *Scale bars,* 100 μm in *A* and *F*; 50 μm in *D* and *E*.

identifying therapeutic strategies against neurodegenerative tauopathies, such as small molecules inhibiting fibrillization of Tau or antibodies blocking the spontaneous cellular uptake of fibril seeds.

Acknowledgments—We thank Anna Stieber for performing immuno-EM in this study; Chi Li for help with molecular cloning; Yuemang Yao and Dr. Michiyo Iba for technical advice on ELISA; Selcuk Tanik and Dr. Laura A. Volpicelli-Daley for valuable suggestions on this study; Drs. Kurt Brunden, Linda Kwong, Kelvin Luk, and John Q. Trojanowski for critical reading of the manuscript; and all the other members of the Center for Neurodegenerative Disease Research for their help and support. mAbs MC-1, PHF1, and Tau 5 are generous gifts from Dr. Peter Davies and Dr. Lester Binder, respectively.

REFERENCES

1. Kosik, K. S., Joachim, C. L., and Selkoe, D. J. (1986) *Proc. Natl. Acad. Sci. U.S.A.* **83,** 4044–4048
2. Pollock, N. J., Mirra, S. S., Binder, L. I., Hansen, L. A., and Wood, J. G. (1986) *Lancet* **2,** 1211
3. Goedert, M., Wischik, C. M., Crowther, R. A., Walker, J. E., and Klug, A. (1988) *Proc. Natl. Acad. Sci. U.S.A.* **85,** 4051–4055
4. Lee, V. M.-Y., Balin, B. J., Otvos, L., Jr., and Trojanowski, J. Q. (1991) *Science* **251,** 675–678
5. Witman, G. B., Cleveland, D. W., Weingarten, M. D., and Kirschner, M. W. (1976) *Proc. Natl. Acad. Sci. U.S.A.* **73,** 4070–4074
6. Drechsel, D. N., Hyman, A. A., Cobb, M. H., and Kirschner, M. W. (1992) *Mol. Biol. Cell* **3,** 1141–1154
7. Biernat, J., Gustke, N., Drewes, G., Mandelkow, E. M., and Mandelkow, E. (1993) *Neuron* **11,** 153–163
8. Bramblett, G. T., Goedert, M., Jakes, R., Merrick, S. E., Trojanowski, J. Q., and Lee, V. M.-Y. (1993) *Neuron* **10,** 1089–1099
9. Goedert, M., Spillantini, M. G., Jakes, R., Rutherford, D., and Crowther, R. A. (1989) *Neuron* **3,** 519–526
10. Andreadis, A., Brown, W. M., and Kosik, K. S. (1992) *Biochemistry* **31,** 10626–10633
11. Kidd, M. (1963) *Nature* **197,** 192–193
12. Berriman, J., Serpell, L. C., Oberg, K. A., Fink, A. L., Goedert, M., and Crowther, R. A. (2003) *Proc. Natl. Acad. Sci. U.S.A.* **100,** 9034–9038
13. Wilcock, G. K., and Esiri, M. M. (1982) *J. Neurol. Sci.* **56,** 343–356
14. Arriagada, P. V., Growdon, J. H., Hedley-Whyte, E. T., and Hyman, B. T. (1992) *Neurology* **42,** 631–639
15. Hutton, M., Lendon, C. L., Rizzu, P., Baker, M., Froelich, S., Houlden, H., Pickering-Brown, S., Chakraverty, S., Isaacs, A., Grover, A., Hackett, J., Adamson, J., Lincoln, S., Dickson, D., Davies, P., Petersen, R. C., Stevens, M., de Graaff, E., Wauters, E., van Baren, J., Hillebrand, M., Joosse, M., Kwon, J. M., Nowotny, P., Che, L. K., Norton, J., Morris, J. C., Reed, L. A., Trojanowski, J., Basun, H., Lannfelt, L., Neystat, M., Fahn, S., Dark, F., Tannenberg, T., Dodd, P. R., Hayward, N., Kwok, J. B., Schofield, P. R., Andreadis, A., Snowden, J., Craufurd, D., Neary, D., Owen, F., Oostra, B. A., Hardy, J., Goate, A., van Swieten, J., Mann, D., Lynch, T., and Heutink, P. (1998) *Nature* **393,** 702–705
16. Spillantini, M. G., Murrell, J. R., Goedert, M., Farlow, M. R., Klug, A., and Ghetti, B. (1998) *Proc. Natl. Acad. Sci. U.S.A.* **95,** 7737–7741
17. Rizzu, P., Van Swieten, J. C., Joosse, M., Hasegawa, M., Stevens, M., Tibben, A., Niermeijer, M. F., Hillebrand, M., Ravid, R., Oostra, B. A., Goedert, M., van Duijn, C. M., and Heutink, P. (1999) *Am. J. Hum. Genet.* **64,** 414–421
18. Goedert, M., and Jakes, R. (2005) *Biochim. Biophys. Acta* **1739,** 240–250
19. Lee, V. M.-Y., Daughenbaugh, R., and Trojanowski, J. Q. (1994) *Neurobiol. Aging* **15,** S87–S89
20. Ballatore, C., Lee, V. M.-Y., and Trojanowski, J. Q. (2007) *Nat. Rev. Neurosci.* **8,** 663–672
21. Kanai, Y., Takemura, R., Oshima, T., Mori, H., Ihara, Y., Yanagisawa, M., Masaki, T., and Hirokawa, N. (1989) *J. Cell Biol.* **109,** 1173–1184
22. Vogelsberg-Ragaglia, V., Bruce, J., Richter-Landsberg, C., Zhang, B., Hong, M., Trojanowski, J. Q., and Lee, V. M.-Y. (2000) *Mol. Biol. Cell* **11,** 4093–4104
23. Goedert, M., Jakes, R., Spillantini, M. G., Hasegawa, M., Smith, M. J., and Crowther, R. A. (1996) *Nature* **383,** 550–553
24. Kampers, T., Friedhoff, P., Biernat, J., Mandelkow, E. M., and Mandelkow, E. (1996) *FEBS Lett.* **399,** 344–349
25. Chirita, C. N., Necula, M., and Kuret, J. (2003) *J. Biol. Chem.* **278,** 25644–25650
26. Wille, H., Drewes, G., Biernat, J., Mandelkow, E. M., and Mandelkow, E. (1992) *J. Cell Biol.* **118,** 573–584
27. Friedhoff, P., von Bergen, M., Mandelkow, E. M., Davies, P., and Mandelkow, E. (1998) *Proc. Natl. Acad. Sci. U.S.A.* **95,** 15712–15717
28. Ren, P. H., Lauckner, J. E., Kachirskaia, I., Heuser, J. E., Melki, R., and Kopito, R. R. (2009) *Nat. Cell Biol.* **11,** 219–225
29. Frost, B., Jacks, R. L., and Diamond, M. I. (2009) *J. Biol. Chem.* **284,** 12845–12852
30. Luk, K. C., Song, C., O'Brien, P., Stieber, A., Branch, J. R., Brunden, K. R., Trojanowski, J. Q., and Lee, V. M.-Y. (2009) *Proc. Natl. Acad. Sci. U.S.A.* **106,** 20051–20056
31. Nonaka, T., Watanabe, S. T., Iwatsubo, T., and Hasegawa, M. (2010) *J. Biol. Chem.* **285,** 34885–34898
32. Clavaguera, F., Bolmont, T., Crowther, R. A., Abramowski, D., Frank, S., Probst, A., Fraser, G., Stalder, A. K., Beibel, M., Staufenbiel, M., Jucker, M., Goedert, M., and Tolnay, M. (2009) *Nat. Cell Biol.* **11,** 909–913
33. de Calignon, A., Fox, L. M., Pitstick, R., Carlson, G. A., Bacskai, B. J., Spires-Jones, T. L., and Hyman, B. T. (2010) *Nature* **464,** 1201–1204
34. Li, W., and Lee, V. M.-Y. (2006) *Biochemistry* **45,** 15692–15701
35. Jicha, G. A., Bowser, R., Kazam, I. G., and Davies, P. (1997) *J. Neurosci. Res.* **48,** 128–132
36. Matsumura, N., Yamazaki, T., and Ihara, Y. (1999) *Am. J. Pathol.* **154,** 1649–1656
37. Gonatas, N. K., and Avrameas, S. (1973) *J. Cell Biol.* **59,** 436–443
38. Broadwell, R. D., Balin, B. J., and Salcman, M. (1988) *Proc. Natl. Acad. Sci. U.S.A.* **85,** 632–636
39. Banks, W. A., Akerstrom, V., and Kastin, A. J. (1998) *J. Cell Sci.* **111,** 533–540
40. Banks, W. A., Kastin, A. J., and Akerstrom, V. (1997) *Life Sci.* **61,** PL119–PL125
41. Khlistunova, I., Biernat, J., Wang, Y., Pickhardt, M., von Bergen, M., Gazova, Z., Mandelkow, E., and Mandelkow, E. M. (2006) *J. Biol. Chem.* **281,** 1205–1214
42. Wang, Y. P., Biernat, J., Pickhardt, M., Mandelkow, E., and Mandelkow, E. M. (2007) *Proc. Natl. Acad. Sci. U.S.A.* **104,** 10252–10257
43. Ferrari, A., Hoerndli, F., Baechi, T., Nitsch, R. M., and Götz, J. (2003) *J. Biol. Chem.* **278,** 40162–40168
44. Sato, S., Tatebayashi, Y., Akagi, T., Chui, D. H., Murayama, M., Miyasaka, T., Planel, E., Tanemura, K., Sun, X., Hashikawa, T., Yoshioka, K., Ishiguro, K., and Takashima, A. (2002) *J. Biol. Chem.* **277,** 42060–42065
45. Bandyopadhyay, B., Li, G., Yin, H., and Kuret, J. (2007) *J. Biol. Chem.* **282,** 16454–16464
46. Hasegawa, M., Smith, M. J., and Goedert, M. (1998) *FEBS Lett.* **437,** 207–210
47. Hong, M., Zhukareva, V., Vogelsberg-Ragaglia, V., Wszolek, Z., Reed, L., Miller, B. I., Geschwind, D. H., Bird, T. D., McKeel, D., Goate, A., Morris, J. C., Wilhelmsen, K. C., Schellenberg, G. D., Trojanowski, J. Q., and Lee, V. M.-Y. (1998) *Science* **282,** 1914–1917
48. Nacharaju, P., Lewis, J., Easson, C., Yen, S., Hackett, J., Hutton, M., and Yen, S. H. (1999) *FEBS Lett.* **447,** 195–199
49. von Bergen, M., Barghorn, S., Li, L., Marx, A., Biernat, J., Mandelkow, E. M., and Mandelkow, E. (2001) *J. Biol. Chem.* **276,** 48165–48174
50. Spillantini, M. G., Crowther, R. A., Kamphorst, W., Heutink, P., and van Swieten, J. C. (1998) *Am. J. Pathol.* **153,** 1359–1363
51. Mirra, S. S., Murrell, J. R., Gearing, M., Spillantini, M. G., Goedert, M., Crowther, R. A., Levey, A. I., Jones, R., Green, J., Shoffner, J. M., Wainer, B. H., Schmidt, M. L., Trojanowski, J. Q., and Ghetti, B. (1999) *J. Neuropathol. Exp. Neurol.* **58,** 335–345
52. van Swieten, J. C., Stevens, M., Rosso, S. M., Rizzu, P., Joosse, M., de

Koning, I., Kamphorst, W., Ravid, R., Spillantini, M. G., and Niermeijer Heutink, P. (1999) *Ann. Neurol.* **46,** 617–626
53. Lewis, J., McGowan, E., Rockwood, J., Melrose, H., Nacharaju, P., Van Slegtenhorst, M., Gwinn-Hardy, K., Paul Murphy, M., Baker, M., Yu, X., Duff, K., Hardy, J., Corral, A., Lin, W. L., Yen, S. H., Dickson, D. W., Davies, P., and Hutton, M. (2000) *Nat. Genet.* **25,** 402–405
54. Götz, J., Chen, F., Barmettler, R., and Nitsch, R. M. (2001) *J. Biol. Chem.* **276,** 529–534
55. Lee, V. M.-Y., Kenyon, T. K., and Trojanowski, J. Q. (2005) *Biochim. Biophys. Acta* **1739,** 251–259
56. Aoyagi, H., Hasegawa, M., and Tamaoka, A. (2007) *J. Biol. Chem.* **282,** 20309–20318
57. Miyasaka, T., Morishima-Kawashima, M., Ravid, R., Kamphorst, W., Nagashima, K., and Ihara, Y. (2001) *J. Neuropathol. Exp. Neurol.* **60,** 872–884
58. Paula-Barbosa, M., Tavares, M. A., and Cadete-Leite, A. (1987) *Brain Res.* **417,** 139–142
59. Hempen, B., and Brion, J. P. (1996) *J. Neuropathol. Exp. Neurol.* **55,** 964–972
60. Boutté, A. M., Neely, M. D., Bird, T. D., Montine, K. S., and Montine, T. J. (2005) *J. Alzheimers Dis.* **8,** 1–6
61. Merrick, S. E., Trojanowski, J. Q., and Lee, V. M.-Y. (1997) *J. Neurosci.* **17,** 5726–5737
62. Zhang, B., Maiti, A., Shively, S., Lakhani, F., McDonald-Jones, G., Bruce, J., Lee, E. B., Xie, S. X., Joyce, S., Li, C., Toleikis, P. M., Lee, V. M.-Y., and Trojanowski, J. Q. (2005) *Proc. Natl. Acad. Sci. U.S.A.* **102,** 227–231
63. Brunden, K. R., Zhang, B., Carroll, J., Yao, Y., Potuzak, J. S., Hogan, A. M., Iba, M., James, M. J., Xie, S. X., Ballatore, C., Smith, A. B., 3rd, Lee, V. M.-Y., and Trojanowski, J. Q. (2010) *J. Neurosci.* **30,** 13861–13866
64. Aguzzi, A., and Rajendran, L. (2009) *Neuron* **64,** 783–790
65. Goedert, M., Clavaguera, F., and Tolnay, M. (2010) *Trends Neurosci.* **33,** 317–325
66. Braak, H., and Braak, E. (1991) *Acta Neuropathol.* **82,** 239–259
67. Asuni, A. A., Boutajangout, A., Quartermain, D., and Sigurdsson, E. M. (2007) *J. Neurosci.* **27,** 9115–9129